D1CH9116 - MMCO
Molecular Modelling applied to organic chemistry

Practical 5: Simulation of the optical properties of organic molecules – absorption

A/ π-π* transition in para-nitroaniline

1/ Configuration Interaction calculation

Optimize the geometry of the para-nitroaniline molecule by performing a configuration interaction calculation at the PM6 level (CI/PM6) with an active space including the two frontier MOs (HOMO and LUMO). Set to 4 the number of final CI eigenstates to be calculated and printed (keyword CISTATE), and calculate the atomic Mulliken charges and dipole moments for all CI eigenstates by checking the option "charge and dipoles" in AGUI (keyword CIDIP). The keyword section of the data file should read as follows:

```
AM1 C.I.=2 CIDIP CISTATE=4 SINGLET TRUSTE T=AUTO VECTORS
```

Check in the output file:

- The symmetry (σ or π) of the frontier orbitals
- The HOMO-LUMO gap
- The dipole moment of the ground state
- The transition energy, wavelength, transition dipole and oscillator strength between the ground and first singlet excited state
- The CI expansion coefficients of the first excited state
- The dipole moment of the first excited state

Results

The HOMO and LUMO are illustrated below. Both have a π symmetry. The HOMO has a larger weight on the donor side (NH2), the LUMO on the acceptor side (NO2).

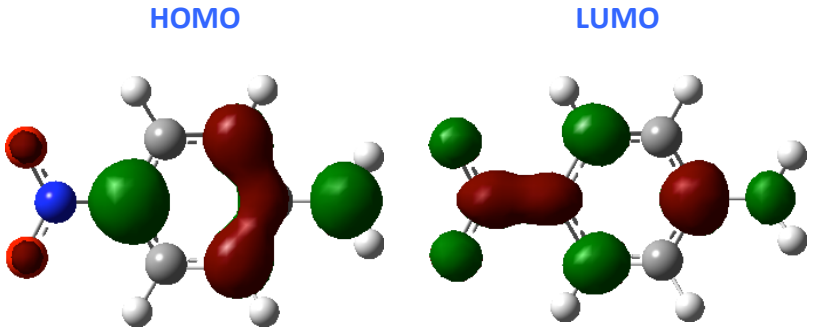

Figure 1: Top view of the frontier orbitals.

The HOMO-LUMO gap amounts to 8.332 eV. The dipole moment is oriented along the C2 molecular axis with a μ(x) component of 8.639 D. The small residual value obtained for μ(z) originates from the slight pyramidalization of the NH2 substituent.

The first spin-allowed electron transition occurs from state 1 to state 3. The associated transition energy, transition dipole moment, oscillator strength and CI expansion coefficients are listed below:

Transition energy / eV	3.987
Transition wavelength / nm	311
Transition dipole moment / D	-2.5445; -0.0147; -0.0259 (components along the Cartesian axis)
Oscillator strength	0.6326
CI expansion coefficients	97% HOMO→LUMO (single) + 3% HOMO→LUMO (double)

We note that HOMO-LUMO gap does not provide a good estimation of the excitation energy.

The x-component of the dipole moment of the first optically active excited state is equal to 12.293 D. The optical excitation leads thus to an increase of the dipole moment of the molecule, which originates from the HOMO-to-LUMO charge transfer, i.e. from the donor to the acceptor moiety.

2/ Description using a 2-state model

a/ Write down the ground and excited state wavefunctions ($|g\rangle$ and $|e\rangle$) of the para-nitroaniline molecule by using a 2-state model implying a neutral form $|N\rangle$ and a zwitterionic form $|Z\rangle$ as basis functions. These latter are orthonormal:

$$\langle N|Z\rangle = \delta_{NZ}$$

The ground and excited state wavefunctions can be expressed as:

$$|g\rangle = \sqrt{(1-\rho)}\,|N\rangle + \sqrt{\rho}\,|Z\rangle$$
$$|e\rangle = \sqrt{\rho}\,|N\rangle - \sqrt{(1-\rho)}\,|Z\rangle$$

with ρ the amount of charge transfer from the donor to the acceptor moiety in the ground state, arising from mesomeric effects:

$$D^{+\rho} \text{—} A^{-\rho}$$

In the excited state, the charge repartition is:

$$D^{+(1-\rho)} \text{—} A^{-(1-\rho)}$$

b/ Build the associated Hamiltonian matrix **H** with elements:

$$\langle N|\hat{H}|Z\rangle = -\sqrt{2}t,\ E_N = \langle N|\hat{H}|N\rangle = 0,\ E_Z = \langle Z|\hat{H}|Z\rangle = 2\eta$$

Hamiltonian matrix in the 2-state basis:

$$\mathbf{H} = \begin{pmatrix} 0 & -\sqrt{2}t \\ -\sqrt{2}t & 2\eta \end{pmatrix}$$

c/ Diagonalize the **H** matrix. Write the energies of the eigenstates and their expansion coefficients in the $\{N,Z\}$ basis as a function of t and η.

$$\begin{cases} \varepsilon_g = \eta\left(1-\sqrt{1+2t^2/\eta^2}\right) \\ \varepsilon_e = \eta\left(1+\sqrt{1+2t^2/\eta^2}\right) \end{cases}$$

$$\rho = \frac{t^2/\eta^2 + 1 - \sqrt{1+2t^2/\eta^2}}{2t^2/\eta^2 + 1 - \sqrt{1+2t^2/\eta^2}}$$

d/ Deduce the expression of the excitation energy ΔE_{ge}, as a function of the parameter ρ measuring the charge transfer between D and A in the ground state. Plot the evolution of ΔE_{ge} with respect to ρ (using t=1.0 eV), and comment.

$$\Delta E_{ge} = \varepsilon_e - \varepsilon_g = 2\sqrt{\eta^2 + 2t^2}$$

$$\Delta E_{ge} = \sqrt{2}t\sqrt{\frac{1}{(1-\rho)\rho}}$$

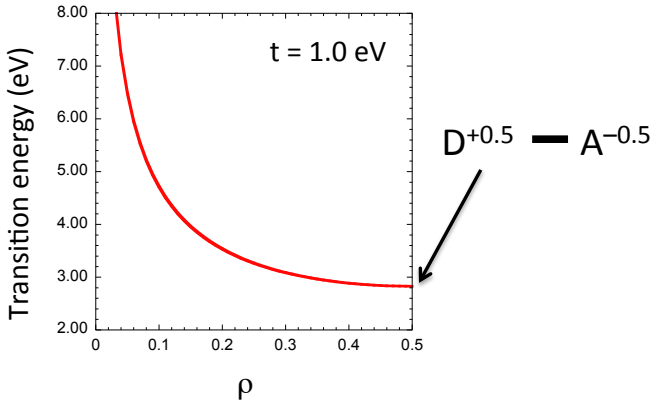

Figure 2: Evolution of ΔE_{ge} with respect to ρ.

Increasing the electron conjugation in the ground state lowers the transition energy.

e/ We consider the dipole moments associated to the $|N\rangle$ and $|Z\rangle$ forms:

$$\mu_N = \langle N|\hat{\mu}|N\rangle = 0$$
$$\mu_Z = \langle Z|\hat{\mu}|Z\rangle = \mu_0$$

Write the expression of the transition dipole moment μ_{ge} along the C_2-symmetry axis between the ground ($|g\rangle$) and excited state ($|e\rangle$) as a function of μ_0 and ρ. Plot the evolution of μ_{ge} with respect to ρ (using μ_0=1.0 D), and comment.

$$\mu_{ge} = \mu_0\sqrt{(1-\rho)\rho}$$
$$f_{ge} \propto \Delta E_{ge}|\mu_{ge}|^2 = \mu_0^2 t\sqrt{2(1-\rho)\rho}$$

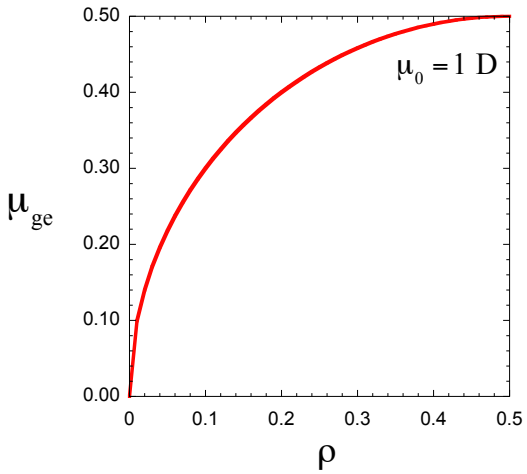

Figure 3: Evolution of μ_{ge} as a function of ρ.

f/ Owing to $f_{ge} \propto \Delta E_{ge}|\mu_{ge}|^2$ deduce the oscillator strength f_{ge} between $|g\rangle$ and $|e\rangle$. Plot the evolution of f_{ge} with respect to ρ (using t=1.0 eV and μ_0=1.0 D), and comment.

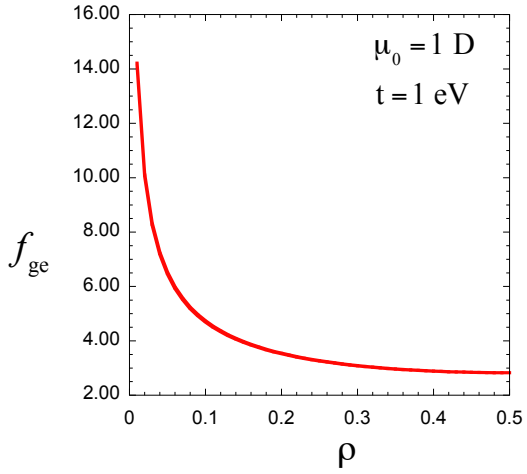

Figure 4: Evolution of f_{ge} as a function of ρ.

3/ Extraction of the effective electronic parameters

By performing a mapping between the electronic eigenstates $|g\rangle$ and $|e\rangle$ obtained in 2/ and the CI eigenstates calculated in 1/, extract the effective electronic parameters t, η and μ_{ge} for the para-nitroaniline molecule.

B/ Impact of the CI active space on the π-π^* transition in para-nitroaniline

1/ SCI within π MOs.

Using the geometry obtained in A, identify the MOs of π symmetry from the LCAO coefficients. Perform a CI calculation at the PM6 level (without relaxing the geometry) including only single excitations (SCI) within the complete set of π orbitals (use the selection tool of AGUI to exclude the σ-orbitals from the active MO space). Check the character of the first allowed excited state (transition energy, oscillator strength and CI expansion coefficients).

The first spin-allowed electron transition occurs from state 1 to state 6. The associated transition energy, transition dipole moment, oscillator strength and CI expansion coefficients are listed below:

Transition energy / eV	3.328
Transition wavelength / nm	373
Transition dipole moment / D	-1.6347; -0.0104; -0.0235 (components along the Cartesian axis)
Oscillator strength	0.2179
CI expansion coefficients	68% H→L + 18% H-1→L+1 + 6% H→L+2 + 2% H-3→L + 2% H-3→L+3

2/ Impact of the number of active MOs.

Perform a series SCI/PM6 calculations on π orbitals while reducing progressively the number of MOs included in the CI process. Check in each case:

- the energy of the ground state
- the number of Slater determinants considered in the CI process
- the character of the first allowed excited state (transition energy, oscillator strength and CI expansion coefficients). *Do not consider electronic states with oscillator strength lower than 0.1*.

The ground state energy provided by SCI calculations is the same as the HF energy (–1755.308318 eV), whatever the size of the SCI active space. In virtue of the Brillouin theorem, single excitations do not couple with the reference HF configuration. Therefore, the ground state energy does not depend on the number of possible single excitations when only those latter are included in the CI process.

The transition energy and oscillator strength associated to the lowest-energy electron transition are reported in Table 1, as a function of the size of the active MO space. The evolution of the transition energy toward the first optically-active excited state with the size of the active MO space is also illustrated Figure 5.

Table 1: Number of Slater determinants included in the CI process, and transition energy (eV) and oscillator strength associated to the lowest-energy electron, as obtained from SCI/PM6 calculations while varying the number of MOs included in the CI process.

Active MO space	Number of Slater determinants	Transition energy / eV	Oscillator strength
SC.I.=2	1	*No excited state* [(a)]	*No excited state* [(a)]
SC.I.=4	7	4.044	0.7328
SC.I.=6	17	3.651	0.2649
SC.I.=8	31	3.483	0.2740
SC.I.=10	49	3.328	0.2179

[(a)] In virtue of the Brillouin theorem, there is no coupling between single excitations and the reference HF state in which all the lowest-energy MOs are doubly occupied. As a consequence, performing a single CI calculation using an active space reduced to two orbitals only does not produce any optically allowed excited state.

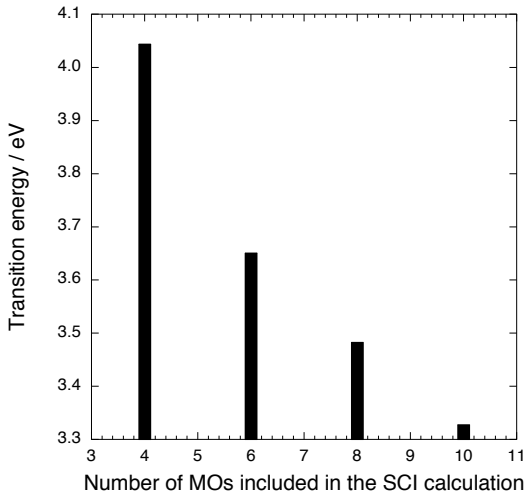

Figure 5: Evolution of ΔE_{ge} as a function of the active MO space.

Both the transition energy and oscillator strength drastically decrease when increasing the number of MOs included in the CI process. As a whole, these results indicate that the calculated optical properties are highly sensitive to the size of the CI active space.

3/ Impact of high-order excitations.

Using the full π-MO space, perform CI calculations including i) single and double excitations (SDCI) and ii) all high-order excitations (*Full* CI). In ii), check the impact of increasing from 1000 to 8000 the maximum number of Slater determinants considered in the CI process, by using the CIMAX keyword. Comment.

The transition energy and oscillator strength associated to the lowest-energy electron transition are reported in Table 2 and 3, for SDCI and full-CI calculations, respectively. The evolution of the transition energy toward the first optically-active excited state with respect to the number of Slater determinants included in the full-CI processes is also illustrated Figure 6.

Table 2: Number of Slater determinants included in the CI process, and transition energy (eV) and oscillator strength associated to the lowest-energy electron, as obtained from a SDCI/PM6 calculation using the full π-MO space.

Active MO space	Number of Slater determinants	Transition energy / eV	Oscillator strength
SC.I.=10	49	3.328	0.2179
SDC.I.=10	805	3.504	0.2608

Compared to single CI calculations, including double excitations leads to an increase of the transition energy toward the first excited state. The reason for this is that, due to their coupling with the reference HF configuration, double excitations do not only impact the first excited state energy, but also stabilize the ground state (the energy of the ground state is reduced by 49 meV compared to that obtained from SCI calculations). Here, this stabilization is larger than the stabilization of the first excited state, which leads to an increase of their energy difference.

Table 3: Number of Slater determinants included in the CI process, and transition energy (eV) and oscillator strength associated to the lowest-energy electron, as obtained from Full-CI calculations at the PM6 level while varying the number of Slater determinants (CIMAX) included in the CI process.

CIMAX	Number of Slater determinants	Transition energy / eV	Oscillator strength
1000	996	3.168	0.2579
2000	1997	3.142	0.2577
3000	2998	3.114	0.2571
4000	3982	3.101	0.2559
5000	4981	3.087	0.2540
6000	5998	3.083	0.2543
7000	6988	3.079	0.2561
8000	7984	3.079	0.2556

As illustrated Figure 6, the transition energy decreases when increasing the number of Slater determinants included in the CI process from 996 to 7984, and converges to the finite value of 3.079 eV. The oscillator strength do not vary significantly.

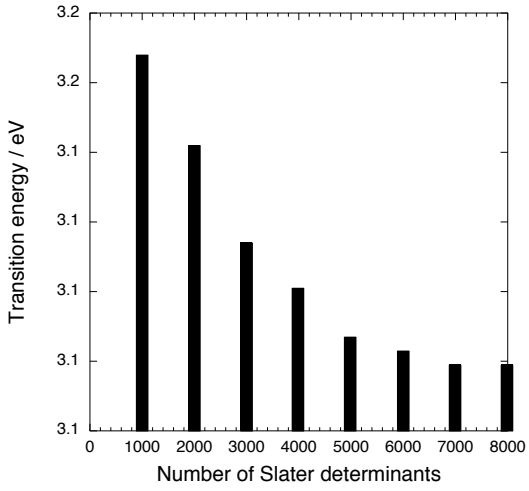

Figure 6: Evolution of ΔE_{ge} as a function of the number of Slater determinants included in the CI process.

C/ Optical properties and conjugation strength

We consider the conjugated push-pull compound schematized below.

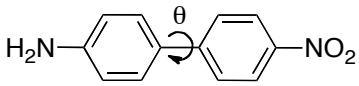

Figure 1: Structure of a push-pull biphenyl derivative

By using the *reaction path* tool of AGUI, run a series of CI calculations at the PM6 level within a minimal HOMO-LUMO active space to investigate the impact of the torsional angle θ on the absorption properties. Comment the results.

The variation of the heat of formation as a function of the torsional angle is plotted Figure 7. The minimal energy structure is obtained for θ = 49°. The evolution of the transition energy and oscillator strength toward the first optically active excited state is illustrated Figure 8. We observe that the transition energy is minimal for the planar structure (θ = 0°), while the associated transition probability is maximal. Increasing θ induces an increase of ΔE_{ge} together with a decrease of f_{ge}. The transition energy reaches a maximum and the oscillator strength vanishes for the structure with the phenyl rings perpendicular (θ = 90°).

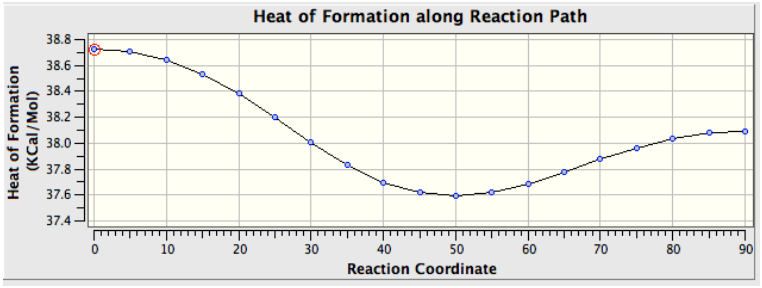

Figure 7: Evolution of the heat of formation as a function of the torsional angle.

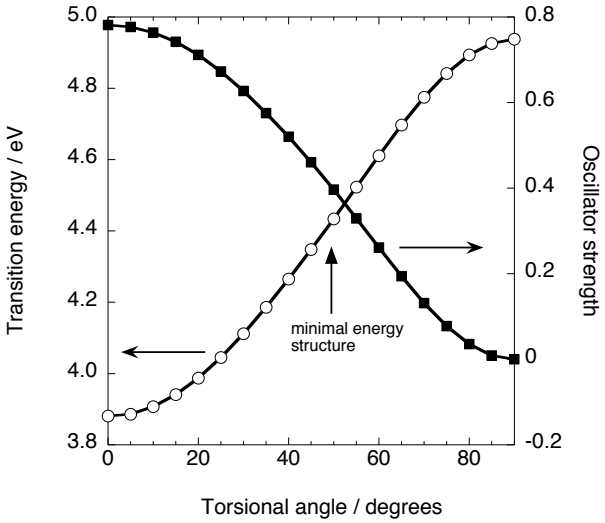

Figure 8: Evolution of ΔE_{ge} and f_{ge} as a function of the torsional angle.

D/ Absorption spectra of model push-pull systems

*Reference TD-DFT calculations of the optical properties of oligothiophene derivatives described in sections 1-2 have been reported in [J. Phys. Chem. C **2012**, 116, 11946–11955].*

1/ Impact of the conjugation length

In this section, we aim to investigate the impact of the length of the conjugated bridge on the optical properties of model a push-pull system schematized below (we consider all-*trans* orientations for the thiophene groups). Build several molecular structures by increasing the number n of thiophene rings from 1 to 10, and optimize their geometry at the SCI/PM6 level while imposing the thiophene chain to remain planar (see the optimization procedure described below). The number of (occupied x vacant) MOs included in the SCI calculations will be defined as (5n x 5n) by using the keyword SC.I.=10n, and all Slater determinants will be considered in the CI process (keyword CIMAX=all). Comment the results.

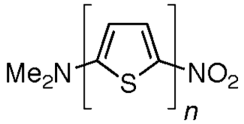

Figure 2: Structure of a model push-pull oligothiophene

Procedure for geometry optimizations:
1 – Optimize the geometrical structure with n=1 at the SCI/PM6 level (SC.I.=10), and check the vibrational frequencies to confirm that you obtained a true minimum.
2 – Build the geometrical structure with n=10, save the .dat file, and set to zero the optimization flags for all dihedrals.
3 – Create the .dat files for structures with 2≤n≤9 from the .dat file generated in step 2.

4 – Run the geometry optimizations for structures with 2≤n≤10 (without calculating vibrational frequencies) by using the following keywords:

```
pm6 sc.i.=10 cistate=10n cimax=all singlet truste
```

Table 4: Transition energy (eV) and oscillator strength to the first allowed excited state as a function of the number n of thiophene rings, as obtained from SCI/PM6 calculations.

n	Transition energy / eV	Oscillator strength
1	3.258	0.4817
2	2.447	0.5476
3	2.226	0.6541
4	2.169	0.8316
5	2.125	1.0097
6	2.101	1.1948
7	2.077	1.3790
8	2.065	1.5704
9	2.049	1.7547
10	2.016	1.8641

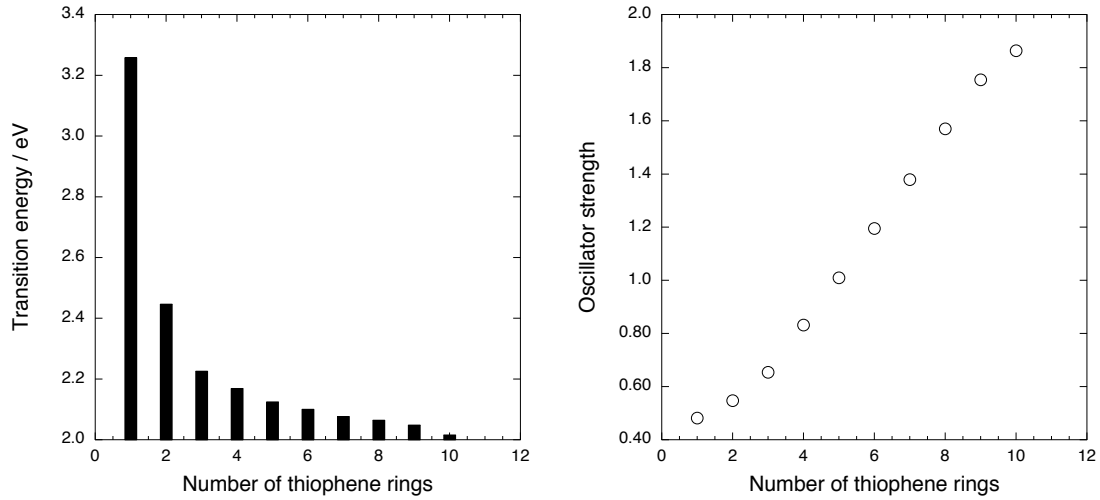

Figure 7: Evolution of ΔE_{ge} (left) and f_{ge} (right) as a function of the number of thiophene rings.

As illustrated Figure 7, the transition energy decreases when increasing the number n of thiophene rings up to a finite value of about 2.0 eV. The oscillator strength evolves quasi linearly with n.

2/ Impact of the donor and acceptor strengths

In this section, we aim to investigate the impact of the terminal electron-donating and electron-withdrawing groups, using a constant central π-conjugated bridge, namely, a pentathiophene segment. Create the .dat files for the two series of push-pull systems below from the optimized structure with n=5 generated in section 1/. Run the geometry optimizations at the SCI(25x25)/PM6 level (keyword SC.I.=50) by using the same

constraint as in Step 1 (planarity of the pentathiophene segment), while fully optimizing the geometry of the new donor/acceptor substituent. Comment the results.

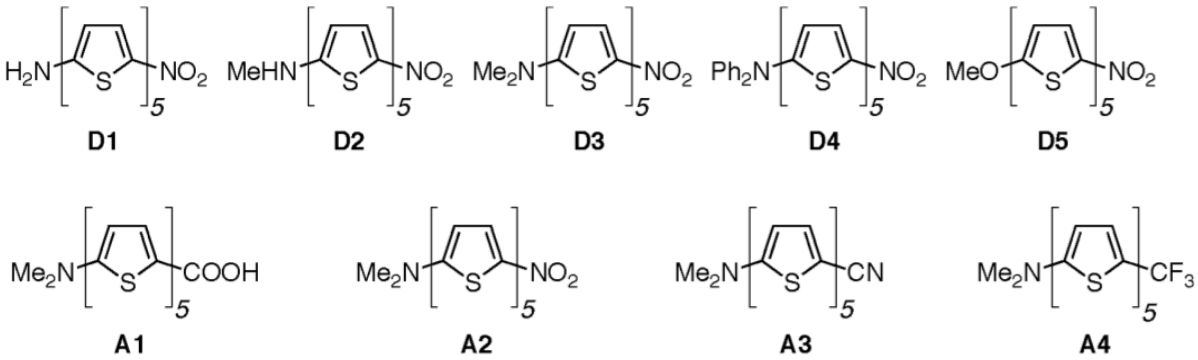

Figure 3: Structure of push-pull pentathiophene derivatives.

The optical features of all derivatives are listed in Table 5. All donors yield virtually the same absorption wavelength (564–576 nm), but it is noticeable that the di-phenyl amino group significantly boost the transition probability. All acceptors yield similar optical properties.

Table 5: Transition energy (eV) and oscillator strength to the first allowed excited state as a function of the number n of thiophene rings, as obtained from SCI/PM6 calculations.

n	Transition energy / eV	Transition wavelength / nm	Oscillator strength
D1	2.177 2.183	570 568	0.1687 0.8042
D2	2.153	576	0.9835
D3	2.125	583	1.0097
D4	2.183	568	1.1453
D5	2.197	564	0.9462
A1	2.147	578	0.9716
A2	2.125	583	1.0097
A3	2.149	577	0.9842
A4	2.144	578	0.9316

3/ A real example: the C212 dye

The most efficient dye-sensitized solar cells (DSCs) actually reported are made of organic-inorganic systems involving a light-harvesting dye molecule anchored onto a mesoporous metal oxide semiconducting film, generally anatase titania (TiO_2), and put into contact with a redox mediator, such as a I^-/I_3^- or Co^{2+}/Co^{3+}-based liquid electrolyte. The C212 dye represented below is prototypical of push-pull molecules used in DSCs.

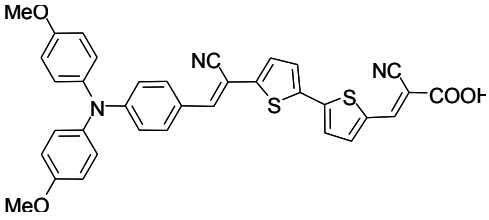

Figure 4: Structure of the C212 dye.

Model the absorption spectrum of the dye at the CI/AM1 level using a (5x5) CI active space and compare to experimental data.

E/ Photochromic systems

We consider below several families of photochromic compounds. Model the absorption spectrum of the two forms at the CI(5x5)/AM1 level. Calculate the displacement of the maximum absorption band along the photochromic reaction.

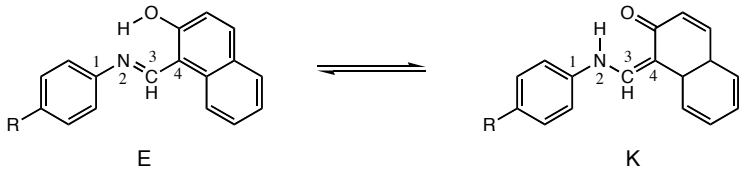

Figure 5: Tautomeric equilibrium of 2-hydroxynaphthaldehyde derivatives

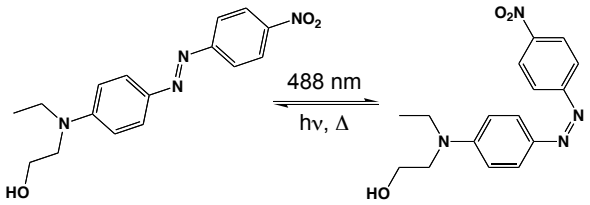

Figure 6: Cis-trans isomerization of Disperse Red 1

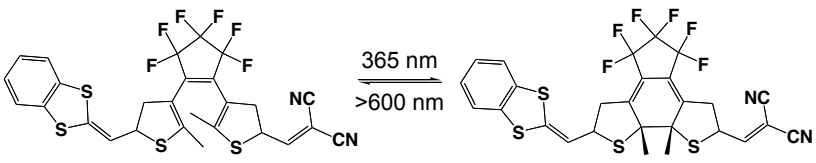

Figure 7: Photochromic equilibrium in a diarylethene derivative